

Local spin polarization by color-field correlators and momentum anisotropy

Haesom Sung,^{1,*} Berndt Müller,^{2,†} and Di-Lun Yang^{1,3,‡}

¹*Institute of Physics, Academia Sinica, Taipei, 11529, Taiwan.*

²*Department of Physics, Duke University, Durham, North Carolina 27708, USA.*

³*Physics Division, National Center for Theoretical Sciences, Taipei, 106319, Taiwan*

We study the local spin polarization of quarks induced by color-field correlators stemming from the correlation of chromo-Lorentz force and chromo-magnetic polarization or chromo-spin Hall effect in the presence of momentum anisotropy. Such effects can trigger longitudinal polarization from fluctuating color fields in glasma or quark gluon plasma phases with transverse expansion for relativistic heavy ion collisions. Especially, from the glasma effect, the resulting longitudinal polarization spectrum of $\Lambda/\bar{\Lambda}$ hyperons has a sinusoidal structure with twice the azimuthal angle relative to the anisotropic direction. An order-of-magnitude estimate of the effect aligns with experimental observations. Our findings highlight the significant role of coherent gluon fields as a novel source for spin polarization phenomena in high-energy nuclear collisions.

Introduction.— Recent experimental findings on the global spin polarization of $\Lambda/\bar{\Lambda}$ hyperons in relativistic heavy ion collisions (HIC) [1, 2] have prompted theoretical investigations into the genesis and transport of quark spin polarization in quark-gluon plasmas (QGP). A widely accepted hypothesis suggests that the substantial angular momentum in peripheral collisions leads to the spin polarization of quarks and gluons via spin-orbit coupling, the polarization subsequently being transferred to hadrons during hadronization and freeze-out [3, 4]. While global thermal equilibrium of hadrons or constituent quarks primarily links their polarization to thermal vorticity [5–7], additional modifications arise under conditions of local equilibrium [8–11].

Particularly, the thermal shear mechanism has been identified as a significant factor in compensating for thermal vorticity, thereby contributing to the generation of longitudinal spin polarization (LSP) along the beam direction [12–17]. This effect yields a sinusoidal angular dependence, specifically with twice the azimuthal angle relative to the reaction plane, which is in qualitative agreement with experimental observations [18]. Nevertheless, the overall sign of LSP, which arises from competing effects, is sensitive to the approximations and input parameters employed. See also Refs. [19, 20] for alternative approaches to address the issue.

Furthermore, recent measurements of LSP in proton-nucleus collisions with high-multiplicity events have revealed a new discrepancy between theoretical predictions [21] and experimental data [22], underscoring the need for incorporating additional effects to fully understand local spin polarization. Despite extensive theoretical endeavors to investigate non-equilibrium effects [23–35] through quantum kinetic theory (QKT) [36–49] and hydrodynamics for spinning fluids [50–59], the underlying mechanisms that can account for the subtle angular structure of LSP with a relevant order of magnitude, beyond the forms in local equilibrium polarization, remain elusive.

On the other hand, the experimentally observed spin alignment for vector mesons in HIC [60, 61] might be

induced by the spin correlation of coalesced quarks and antiquarks produced by strong-force fields such as the fluctuating vector-meson fields [62–64] or glasma fields and color fields from low-energy thermal gluons in QGP [65–67]. One can ask under what conditions such gluonic contributions could influence the polarization of quarks in connection to the LSP of $\Lambda/\bar{\Lambda}$ hyperons, which can reveal the microscopic features of QCD matter created from HIC.

In this letter, we employ QKT for massive quarks in the presence of background color fields [68, 69] to derive the spin polarization spectrum. This spectrum is induced by color-field correlators, with the momentum anisotropy being characterized by the quark flow velocity. These color-field correlators originate from the intricate correlations involving the chromo-Lorentz force, chromo-magnetic polarization, or the chromo-spin Hall effect, without necessitating the assumption of local equilibrium for spin degrees of freedom. In fact, a similar phenomenon was reported in Refs. [68, 69], where spin polarization could only be generated by the parity-odd correlator between chromo-electric and chromo-magnetic fields in the absence of anisotropic flow.

We demonstrate in this Letter that parity-even correlators, arising from pairs of chromo-magnetic or chromo-electric fields, also induce polarization in the presence of collective flow. We show that this mechanism naturally gives rise to the sinusoidal angular structure observed in LSP. We further estimate the order of magnitude for LSP from color fields led by glasma and QGP phases where the fields are, respectively, longitudinally dominant or isotropic. The effects from the two phases are found to be competing with each other due to the subtlety of the freeze-out hypersurface. Finally, we discuss the significance of these findings particularly in the context of high-multiplicity proton-nucleus collisions.

Throughout this Letter, we use the mostly minus signature of the Minkowski metric $\eta^{\mu\nu} = \text{diag}(1, -1, -1, -1)$ and the completely antisymmetric tensor $\epsilon^{\mu\nu\rho\lambda}$ with $\epsilon^{0123} = 1$. We use the notations $A^{(\mu}B^{\nu)} \equiv A^\mu B^\nu + A^\nu B^\mu$

and $A^{[\mu}B^{\nu]} \equiv A^\mu B^\nu - A^\nu B^\mu$ and also define $\tilde{F}^{\alpha\mu\nu} \equiv \epsilon^{\mu\nu\alpha\beta} F_{\alpha\beta}^a/2$ with $F^{a\mu\nu}$ being the field strength of color fields and the upper index a representing color. The chromo-electric and chromo-magnetic fields are explicitly given by $F_{\mu\nu}^a = -\epsilon_{\mu\nu\alpha\beta} B^{a\alpha} \bar{n}^\beta + E_{[\mu}^a \bar{n}_{\nu]}$, where $\bar{n}^\mu = (1, \mathbf{0})$ denotes the temporal direction.

Spin polarization from color-field correlators.— Before introducing QKT, we provide an intuitive argument for generating spin polarization from color fields. We consider the chromo-Lorentz force, $\mathbf{F}^a = g(\mathbf{E}^a + \mathbf{u} \times \mathbf{B}^a)$, and the color-octet polarization pseudo-vector from chromo-magnetic polarization and chromo-spin Hall effect, $\mathbf{P}^a = g(\mathbf{B}^a - \mathbf{u} \times \mathbf{E}^a)$, for the quark transport, where \mathbf{u} as a flow velocity delineates momentum anisotropy. The color-singlet polarization pseudo-vector for quarks with momentum \mathbf{p} can accordingly be constructed by the correlation, $\langle (\mathbf{p} \cdot \mathbf{F}^a) \mathbf{P}^a \rangle \sim (\mathbf{p} \times \mathbf{u}) (\langle \mathbf{B}^a \cdot \mathbf{B}^a \rangle + \langle \mathbf{E}^a \cdot \mathbf{E}^a \rangle)$, when having just non-vanishing parity-even color-field correlators. Here we have introduced $\langle \rangle$ to denote the ensemble average over color sources. We now derive this effect in the QKT.

We start with an outline for essential steps in the derivation of the spin polarization spectrum of quarks with background color fields constructed in Ref. [68, 69]. In general, the building blocks of the spin polarization spectrum are the vector and axial-vector components of Wigner functions for massive fermions, $\mathcal{V}^\mu(p, x)$ and $\mathcal{A}^\mu(p, x)$, responsible for the particle-number and spin-current density in phase space, respectively. For quarks carrying color charges, they can be further decomposed into the color-singlet and color-octet components,

$$\begin{aligned} \mathcal{V}^\mu(p, x) &= \mathcal{V}^{s\mu}(p, x)I + \mathcal{V}^{a\mu}(p, x)t^a, \\ \mathcal{A}^\mu(p, x) &= \mathcal{A}^{s\mu}(p, x)I + \mathcal{A}^{a\mu}(p, x)t^a, \end{aligned} \quad (1)$$

where t^a are the $SU(N_c)$ generators such that $[t^a, t^b] = if^{abc}t^c$ and $\{t^a, t^b\} = N_c^{-1}\delta^{ab}I + d^{abc}t^c$ and I is the identity matrix in color space. Assuming the spin of Λ hyperons is primarily dictated by the spin of strange quark therein (and same for the $\bar{\Lambda}$ and strange antiquark) and the perfect transition of the polarization from quarks to hadrons, known as the strange-equilibrium scenario [12, 14], the polarization spectrum of Λ hyperons is given by

$$\mathcal{P}^\mu(\mathbf{p}) = \frac{\text{tr}_c \left[\int d\Sigma \cdot p \mathcal{A}^\mu(\mathbf{p}, x) \right]}{2M_\Lambda \text{tr}_c \left[\int d\Sigma \cdot \mathcal{V}(\mathbf{p}, x) \right]}, \quad (2)$$

where $\mathcal{A}^\mu(\mathbf{p}, x) \equiv (2\pi)^{-1} \int dp_0 \mathcal{A}^\mu(p, x)$ and $\mathcal{V}^\mu(\mathbf{p}, x) \equiv (2\pi)^{-1} \int dp_0 \mathcal{V}^\mu(p, x)$ as the onshell Wigner functions and $d\Sigma^\mu$ denotes the normal vector of a spin freeze-out hypersurface. Here M_Λ corresponds to the mass of Λ hyperons in light of the phenomenological choice for normalization. Since tr_c as the trace over color space is taken, we will focus on the color-singlet components contributing to $\mathcal{P}^\mu(\mathbf{p})$.

Based on the quantum nature of spin, we adopt the power counting, $\mathcal{V}^\mu \sim \mathcal{O}(\hbar^0)$ and $\mathcal{A}^\mu \sim \mathcal{O}(\hbar)$ in the \hbar expansion as the gradient expansion in phase space [45, 49], and consider the leading-order contributions led by

$$\mathcal{V}^{s\mu}(\mathbf{p}, x) = \left(\frac{p^\mu}{2p_0} f_V^s(p, x) \right)_{p_0=\epsilon_{\mathbf{p}}} \quad (3)$$

and

$$\begin{aligned} \mathcal{A}^{s\mu}(\mathbf{p}, x) &= \frac{1}{2\epsilon_{\mathbf{p}}} \left[\tilde{a}^{s\mu}(p, x) - \frac{\hbar g}{4N_c} \tilde{F}^{a\mu\nu}(x) \partial_{p\nu} f_V^a(p, x) \right]_{p_0=\epsilon_{\mathbf{p}}} \\ &\quad + \frac{\hbar g}{8N_c} \tilde{F}^{a\mu\nu}(x) \partial_{p_\perp\nu} (f_V^a(p, x)/\epsilon_{\mathbf{p}})_{p_0=\epsilon_{\mathbf{p}}}, \end{aligned} \quad (4)$$

where $\epsilon_{\mathbf{p}} \equiv \sqrt{\mathbf{p}^2 + m^2}$ and $p_{\perp\nu} \equiv p_\nu - p_0 \bar{n}_\nu$. We also introduce $\partial_{V\mu} \equiv \partial/\partial V^\mu$ and $\partial_V^\mu \equiv \partial/\partial V_\mu$. Here $f_V^s(p, x)$ and $f_V^a(p, x)$ denote the color-singlet and color-octet vector-charge distribution functions, respectively. Analogously, $\tilde{a}^{s\mu}(p, x)$ represents the color-singlet effective spin four-vector in phase space, while its color-octet counterpart is of higher orders in $\mathcal{V}^{s\mu}(\mathbf{p}, x)$ and neglected here. In a QCD medium, $f_V^a(p, x)$ originates from color fluctuations induced by color fields and given $f_V^s(p, x)$. The $\tilde{F}^{a\mu\nu}$ terms in Eq. (4) are responsible for chromo-magnetic polarization and the chromo-spin Hall effect.

The dynamical evolution of the vector-charge distribution functions and effective spin four-vectors are governed by kinetic equations. For weakly coupled systems with slow-varying color fields, dynamical polarization led by non-vanishing $\tilde{a}^{s\mu}(p, x)$ is suppressed and we will simply focus on the non-dynamical polarization from the remaining terms of Eq. (4). At weak coupling, $f_V^a(p, x)$ can be solved from the collisionless color-octet Vlasov equation perturbatively as the quark evolution under chromo-Lorentz force,

$$f_V^a(p, x) = -\frac{g}{p_0} \int_{t_i}^{x_0} dx'_0 p'^\mu F_{\nu\mu}^a(x') \partial_p^\nu f_V^s(p, x') \Big|_c, \quad (5)$$

where $|_c = \{x_{\text{T}}^i = x_{\text{T}}^i, x_{\parallel}^i = x_{\parallel}^i - p^i(x_0 - x'_0)/p_0\}$ with x_0 being the present time and $t_i \leq x_0$ denotes an initial time when color fields affect the quark transport. The subscripts, T and \parallel , are utilized to represent the components transverse and parallel to \mathbf{p} . One hence finds

$$\begin{aligned} \mathcal{A}^{s\mu}(\mathbf{p}, x) &= \left[\frac{\hbar g^2}{8p_0 N_c} \int_{t_i}^{x_0} dx'_0 \langle \tilde{F}^{a\mu\nu}(x) F_{\alpha\beta}^a(x') \rangle \right. \\ &\quad \left. \times \mathcal{D}_{p\nu} \left(p^\beta \partial_p^\alpha f_V^s(p, x') \right) \right] \Big|_c \Big|_{p_0=\epsilon_{\mathbf{p}}}, \end{aligned} \quad (6)$$

where

$$\mathcal{D}_{p\nu} \equiv \partial_{p\nu} p_0^{-1} - \epsilon_{\mathbf{p}} \partial_{p_\perp\nu} \epsilon_{\mathbf{p}}^{-2} + p_{\perp\nu} \epsilon_{\mathbf{p}}^{-2} \partial_{p_0}. \quad (7)$$

For a more detailed derivation we refer to Refs. [68, 69].

Standard phenomenology of relativistic HIC suggests that the quarks undergo transverse expansion and their

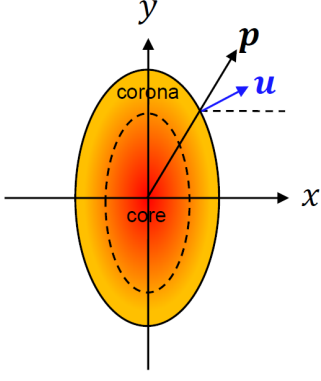


FIG. 1. A schematic figure for the transverse plane of the QCD medium (glasma or QGP), where the region inside the dashed ellipse represents the core, while the region between the solid ellipse and the dashed one corresponds to the corona. Also, \mathbf{u} and \mathbf{p} denote the flow velocity and momentum of the quark on the medium surface.

momentum spectrum depends on $p \cdot u / \Lambda_c$, where u^μ is a local collective velocity field and Λ_c is a typical scale of the medium. In the early collision stage this transverse flow is thought to be generated by glasma fields [70]; in the QGP stage it is governed by hydrodynamics.

When taking t_i close to x_0 and assuming slowly varying color-field correlators, Eq. (6) can be approximated as

$$\mathcal{A}^{s\mu}(\mathbf{p}, x) \approx \frac{\hbar g^2 \Delta t}{8\epsilon_{\mathbf{p}} N_c} (\tilde{F}^{\alpha\mu\nu}(x) F^{\alpha\beta}(x)) u_\alpha \left(\hat{O}_{\nu\beta}^{(2)} \partial_{p \cdot u}^2 + \frac{1}{\epsilon_{\mathbf{p}}} \hat{O}_{\nu\beta}^{(1)} \partial_{p \cdot u} \right) f_V^s \left(\frac{p \cdot u}{\Lambda_c} \right) \Big|_{p_0 = \epsilon_{\mathbf{p}}}, \quad (8)$$

where $\hat{O}_{\nu\beta}^{(2)} = u_0 p_\nu p_\beta / \epsilon_{\mathbf{p}}^2$, $\hat{O}_{\nu\beta}^{(1)} = p_{(\nu} \bar{n}_{\beta)} / \epsilon_{\mathbf{p}} - 2p_\nu p_\beta / \epsilon_{\mathbf{p}}^2$ and $\Delta t = x_0 - t_i$. As indicated earlier, we here consider only parity-even correlators for paired chromo-electric fields and chromo-magnetic fields: $\langle E^i(x) E^j(x) \rangle = \delta^{ij} \langle E^i(x) E^i(x) \rangle$, $\langle B^i(x) B^j(x) \rangle = \delta^{ij} \langle B^i(x) B^i(x) \rangle$, and $\langle E^i(x) B^j(x) \rangle = 0$. Selecting z as the longitudinal direction, Eq. (8) then reduces to

$$\mathcal{A}^{sz}(\mathbf{p}, x) \approx \frac{\hbar g^2 \Delta t}{8\epsilon_{\mathbf{p}}^2 N_c} (\langle B_z^a(x) B_z^a(x) \rangle + \langle E_T^a(x) E_T^a(x) \rangle) \epsilon^{zjk} p^j u^k (u^0 \partial_{p \cdot u} - \epsilon_{\mathbf{p}}^{-1}) \partial_{p \cdot u} f_V^s \left(\frac{p \cdot u}{\Lambda_c} \right) \Big|_{p_0 = \epsilon_{\mathbf{p}}}, \quad (9)$$

where we have imposed rotational symmetry on the correlator of transverse color fields E_T^a . Notwithstanding the weak coupling assumption, our derivation should capture the generic form of $\mathcal{A}^{sz}(\mathbf{p}, x)$ up to linear order in the color-field correlators. Equation (9) manifests the angular structure, $\mathcal{P}^z \sim (\mathbf{u} \times \mathbf{p})^z$, for LSP, whereas the overall sign will also depend on the freeze-out hypersurface.

Polarization from glasma.— In early times of high-energy nuclear collisions, the overpopulated gluons may

be described by classical chromo-electromagnetic fields in the color glass condensate effective theory [71–75] and form the so-called glasma phase [76, 77]. We may now employ Eq. (9) to study the LSP induced by glasma fields with an initial flow. To make a more systematic estimate of the polarization spectrum, we shall take into account the integral over a freeze-out hypersurface. We consider the isochronous freeze-out in 3+1 dimensions at fixed $\tilde{\tau} = \tilde{\tau}_f$ with $\tilde{\tau} \equiv \sqrt{\tau^2 - x^2 - y^2} = \sqrt{t^2 - x^2 - y^2 - z^2}$. To further delineate the elliptical asymmetry of the transverse plane, we parameterize

$$x = r\sqrt{1 - \epsilon} \cos \Phi, \quad y = r\sqrt{1 + \epsilon} \sin \Phi, \quad (10)$$

where ϵ as a model parameter represents the elongation along the y axis and $r \leq r_m$ characterizes the transverse size of the medium. The four-momentum is parameterized as

$$p^\mu = (\epsilon_T \cosh y_p, p_T \cos \phi, p_T \sin \phi, \epsilon_T \sinh y_p), \quad (11)$$

where $\epsilon_T \equiv \sqrt{m^2 + p_T^2}$ and y_p denotes the momentum rapidity. Based on e.g., Refs. [78, 79], it is found

$$d\Sigma \cdot p = dr d\Phi d\eta r \sqrt{1 - \epsilon^2} (G_1 \cosh(y_p - \eta) + G_2), \quad (12)$$

where

$$G_1 = \sqrt{(m^2 + p_T^2)} \tau_f, \quad G_2 = -(xp^x + yp^y), \quad (13)$$

with $\tau_f(x, y) = \sqrt{\tilde{\tau}_f^2 + x^2 + y^2}$. Without the loss of generality for semi-quantitative estimates, we may parameterize the four velocity as

$$u^\mu = \frac{1}{N_v} (1, v^x, v^y, 0), \quad (14)$$

where $N_v = \sqrt{1 - v_x^2 - v_y^2}$ with

$$v^x = u_T (1 + \delta) \frac{x_T}{r_m^2}, \quad v^y = u_T (1 - \delta) \frac{y_T}{r_m^2}. \quad (15)$$

Here u_T and δ are model parameters characterizing the strength and anisotropy of flow. Such initial flow may be induced by pressure gradients of glasma [80, 81].

We first focus on the contribution from the corona of the glasma as depicted in Fig. (1), for which the quarks may immediately hadronize after the glasma phase without thermalizing as opposed to the quarks from the core that will further go through the QGP phase before hadronization. In the glasma phase, the longitudinal color fields are supposed to be more dominant. We hence omit the correlator from transverse chromo-electric fields and neglect the time evolution of color fields in the corona. To make an order-of-magnitude estimate, we adopt the Golec-Biernat Wüsthoff (GBW) dipole distribution [82, 83] to approximate

$$g^2 \langle B^{az}(t_i) B^{az}(t_i) \rangle \approx \frac{(N_c^2 - 1)}{2N_c} Q_s^4, \quad (16)$$

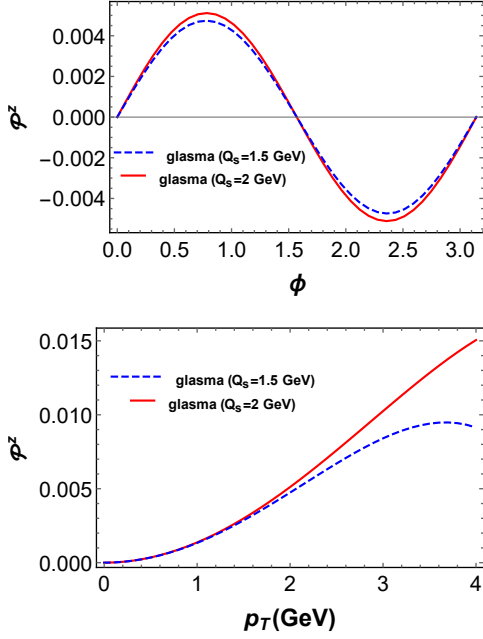


FIG. 2. \mathcal{P}^z at $y_p = 0$ from glasma and Eq. (17) for quark distributions. The upper panel shows ϕ dependence with $p_T = 2$ GeV and the lower shows p_T dependence with $\phi = \pi/4$. The blue dashed and red solid curves correspond to $Q_s = 1.5$ GeV and $Q_s = 2$ GeV, respectively.

where Q_s denotes the saturation scale. We postulate two types of quark distributions in glasma. One characterizes the Schwinger pair production by chromo-electric fields in early times¹,

$$f_V^s(p \cdot u/Q_s) = e^{-\pi(p \cdot u)^2/|gE^a|} \quad (17)$$

with $|gE^a| \approx \sqrt{(N_c^2 - 1)/(2N_c)}Q_s^2$ based on the GBW distribution. Another is a quasi-equilibrium form for quarks at relatively late times in the glasma,

$$f_V^s(p \cdot u/Q_s) = \frac{1}{e^{p \cdot u/Q_s} + c}, \quad (18)$$

eventually approaching thermal equilibrium characterized by $Q_s \rightarrow T$ and $c \rightarrow 1$. Here we set $0 \leq c \leq 1$ to describe the overpopulation of quarks driven by the high density of gluons at low energy while satisfying the Pauli exclusion principle. We then evaluate the LSP via

$$\begin{aligned} \mathcal{P}^z \approx & \frac{\hbar(N_c^2 - 1)Q_s^2 \Delta t}{16M_\Lambda N_c^2 \epsilon_p} \int d\Sigma \cdot p f_V^s \int d\Sigma \cdot p (p^x u^y - p^y u^x) \\ & \times (u^0 \partial_{p \cdot u/Q_s} - Q_s/\epsilon_p) \partial_{p \cdot u/Q_s} f_V^s. \end{aligned} \quad (19)$$

¹ The original pair production rate is given by $\Gamma \sim e^{-\pi m^2/|eE|}$ [84]. Here we simply make the generalization to replace m by $p \cdot u$ to capture the momentum anisotropy of produced quarks and $|eE|$ by $|gE^a|$. See Refs. [85–89] for follow-up studies of the Schwinger mechanism by chromo-electric fields.

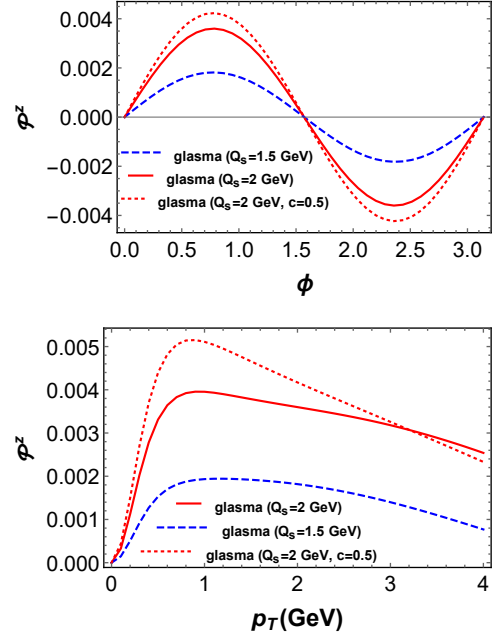


FIG. 3. \mathcal{P}^z at $y_p = 0$ from glasma and Eq. (18) for quark distributions. The same color assignment as Fig. 2 for $c = 1$. The additional red dotted curves represent the cases with $Q_s = 2$ GeV and $c = 0.5$ for comparisons.

We consider $\epsilon = 0$ and a weak initial flow with $u_T \ll 1$ such that $|p \cdot u| \ll Q_s$, whereby f_V^s and N_v are almost Φ independent. In such a case, the contribution from G_2 in $\int d\Sigma \cdot p u^{[y} p^{x]} u^0$ becomes dominant, which results in

$$\int d\Sigma \cdot p u^{[y} p^{x]} u^0 \approx u_T p_T^2 \pi \sin 2\phi \int \frac{dr d\eta r^3 \tau \delta}{r_m^2} \quad (20)$$

and consequently the $\sin 2\phi$ structure is manifested. We note that the polarization vanishes for isotropic flow, $\delta = 0$ as expected.

We have numerically evaluated Eq. (19) by integrating over $r_m - \Delta t \leq r \leq r_m$, $0 \leq \Phi \leq 2\pi$, and $-1 \leq \eta \leq 1$ at a fixed $\tilde{\tau}_f$, where the regime $r_m - \Delta t \leq r \leq r_m$ is set to capture only the corona contribution. Here we focus on the case with $\tilde{\tau}_f \approx 0$ such that $\tau_f \approx r \leq r_m$. We take $\hbar = 1$, $N_c = 3$, $m = 0.5$ GeV as the constituent strange quark mass, $M_\Lambda = 1.12$ GeV, $\Delta t = 0.2$ fm and $r_m \approx \tau_f^{\max} = 0.5$ fm as the typical time scale smaller than 1 fm for glasma phase. We set $\delta = 0.3$ by analogy with the anisotropy parameter adopted in the thermal model for non-central collisions [79, 90], while we take $u_T = 0.01$ and $u_T = 0.2$ for Eq. (17) and Eq. (18) characterizing the initial and final quark distributions in the glasma phase, respectively, as the weak non-equilibrium flow gradually generated by pressure gradients of glasma in time. The ϕ dependence of \mathcal{P}^z at fixed $p_T = 2$ GeV for $Q_s = 1.5$ or 2 GeV are shown in Fig. 2 and Fig. 3, where the $\sin 2\phi$ structure is observed as anticipated. In addition, \mathcal{P}^z with transverse-momentum dependence at fixed $\phi = \pi/4$ is also presented therein. For large p_T , the G_1 contribution

becomes more substantial when $|\mathbf{p} \cdot \mathbf{u}| \sim Q_s$, which may cause the sign flipping of \mathcal{P}^z at sufficiently large p_T .

Polarization from quark gluon plasma.— One may similarly consider LSP engendered by isotropic color fields coming from the soft thermal gluons in QGP. For more realistic setup of the flow profile, we may employ the thermal model with single freeze-out for HIC [91]. Following this approach, we set

$$u^\mu = \frac{1}{N_u} (t, x\sqrt{1+\delta}, y\sqrt{1-\delta}, z), \quad (21)$$

where $N_u = \sqrt{\tilde{\tau}^2 - (x^2 - y^2)\delta}$ and δ again is a model parameter delineating the transverse anisotropy of the flow. For the isotropic color-field correlators, we approximate $\langle B_z^a(x)B_z^a(x) \rangle \approx \langle E_T^a(x)E_T^a(x) \rangle \approx T^4$ albeit more rigorous estimation needed. Then, we may evaluate \mathcal{P}^z by simply multiplying Eq. (19) by $4g^2N_c/(N_c^2 - 1)$ and replacing Q_s with T and adopt the Fermi-Dirac distribution for quarks, while now integrating over the range $0 \leq r \leq r_m$.

Following Refs. [79, 90] for fitting the hadron spectra and flow of Au-Au collisions at $\sqrt{s_{NN}} = 130$ GeV, we take $\epsilon = 0.055$, $\delta = 0.12$, $\tilde{\tau}_f = 7.7$ fm, and $r_m = 6.5$ fm for 0–15% centrality and $\epsilon = 0.137$, $\delta = 0.37$, $\tilde{\tau}_f = 4.3$ fm, and $r_m = 3.8$ fm for 30–60% centrality, respectively. We also adopt $T = T_f = 165$ MeV as the freeze-out temperature, $g = \sqrt{4\pi/3}$, and $\Delta t = 0.2$ fm on an equal footing to glasma (also such that T_f is approximately constant). The ϕ and p_T dependence for \mathcal{P}^z are shown in Fig. 4. Since now $|\mathbf{p} \cdot \mathbf{u}| \gg T_f$, the G_1 contribution dominates and the overall sign of \mathcal{P}^z is opposite with respect to the glasma case, while the $\sin 2\phi$ structure remains. However, the overall magnitude here could have larger uncertainties subject to chosen parameters. We only emphasize the qualitative difference with the glasma case.

Discussions and summary.— Overall, the sign and azimuthal-angle dependence of \mathcal{P}^z obtained from glasma fields are consistent with present experimental observations [18, 22]. Although more sophisticated modeling is needed to quantify \mathcal{P}^z , our rough order-of-magnitude estimate for $\mathcal{P}^z \sim 0.1 - 1\%$ is also comparable to the measurements. In practice, we expect that the observed polarization has contributions from both the glasma (corona) and QGP (core). Accordingly, the total degree of polarization may be expressed as

$$\mathcal{P}^z = \frac{N_{\text{GL}}\mathcal{P}_{\text{GL}}^z + N_{\text{QGP}}\mathcal{P}_{\text{QGP}}^z}{N_{\text{GL}} + N_{\text{QGP}}}, \quad (22)$$

where N denotes the particle number and the subscripts GL and QGP represent the contributions from the glasma (corona) and QGP (core), respectively. In general, N_{GL} and N_{QGP} should be more dominant at high p_T for small systems and at low p_T for large systems, respectively. More sophisticated modeling and simulations for the core

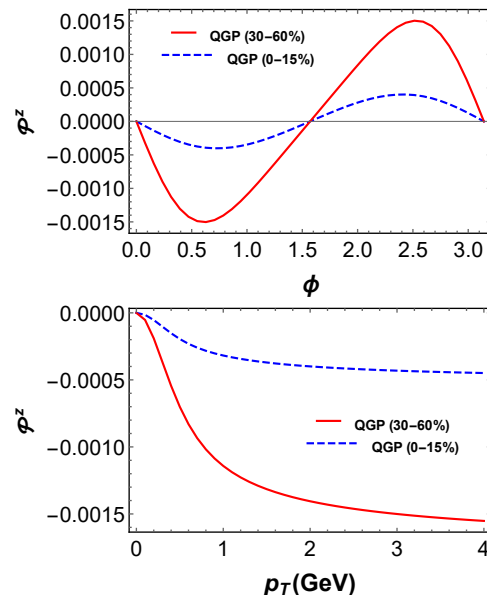


FIG. 4. \mathcal{P}^z at $y_p = 0$ from QGP. The upper panel shows ϕ dependence with $p_T = 2$ GeV and the lower shows p_T dependence with $\phi = \pi/4$. The blue dashed and red solid curves correspond to 0–15% centrality and 30–60% centrality, respectively.

and corona scenario similar to Ref. [92] will be needed to quantify the results. Despite the dependence on transverse momenta and centrality, it is found therein that the corona contribution for hadron yields is about 50% when the multiplicity per rapidity reaches $\mathcal{O}(10^1)$ for both p+p and Pb+Pb collisions. For a heuristic estimation, by taking $\mathcal{P}_{\text{GL}}^z = 4 \times 10^{-3}$ and $\mathcal{P}_{\text{QGP}}^z = -1.5 \times 10^{-3}$ from Fig. 2 and Fig. 4, Eq. (22) still yields $\mathcal{P}^z \approx 0.1\%$ for multiplicity around tens to a few hundreds as for small collision systems.

Recent measured strength of \mathcal{P}^z in proton-nucleus collisions at LHC shows a mild opposite trend against multiplicity [22], which could be qualitatively explained by the substantial contribution from the corona in smaller collision systems due to the suppression of N_{QGP} with lower multiplicity. When the local equilibrium condition for spin degrees of freedom is reached, there exist additional contributions from thermal vorticity and thermal-shear corrections for $\mathcal{P}_{\text{QGP}}^z$, further competing with the glasma effect. Finally, we remark that the initial flow for quarks in glasma could also stem from mini-jets and thus the momentum anisotropy and hydrodynamic flow may be misaligned with increasing multiplicity.

In conclusion, we have shown that the correlators of color fields can create local spin polarization in the presence of anisotropic flow. We further argued that this mechanism can qualitatively explain the LSP of $\Lambda/\bar{\Lambda}$ hyperons in high-energy nuclear collisions from the glasma fields in corona, especially for small collision systems, while the polarization could be partially modified by the

thermal color fields or hydrodynamic effects in QGP. Our findings demonstrate the possible significant influence of gluons on spin transport of quarks in HIC and complement the studies on spin alignment of vector mesons by strong forces [62–67]. Extending previous applications of QCD effective kinetic theory [93–95] to derive the initial conditions for hydrodynamics, our approach could provide the initial conditions for spin transport theories in the QGP such as spin hydrodynamics [52, 96].

Acknowledgments. D.-L. Y. thanks A. Kumar for useful discussions. This work was supported by a grant from the U. S. Department of Energy, Office of Science (DE-FG02-05ER41367), by National Science and Technology Council (Taiwan) under Grant No. NSTC 113-2628-M-001-009-MY4, and by Academia Sinica under Project No. AS-CDA-114-M01.

* ioussom@gmail.com

† bmueller@duke.edu

‡ dilunyang@gmail.com

- [1] L. Adamczyk *et al.* (STAR), Global Λ hyperon polarization in nuclear collisions: evidence for the most vortical fluid, *Nature* **548**, 62 (2017), arXiv:1701.06657 [nucl-ex].
- [2] J. Adam *et al.* (STAR), Global polarization of Λ hyperons in Au+Au collisions at $\sqrt{s_{NN}} = 200$ GeV, *Phys. Rev. C* **98**, 014910 (2018), arXiv:1805.04400 [nucl-ex].
- [3] Z.-T. Liang and X.-N. Wang, Globally polarized quark-gluon plasma in non-central A+A collisions, *Phys. Rev. Lett.* **94**, 102301 (2005), [Erratum: *Phys. Rev. Lett.* 96,039901(2006)], arXiv:nucl-th/0410079 [nucl-th].
- [4] Z.-T. Liang and X.-N. Wang, Spin alignment of vector mesons in non-central A+A collisions, *Phys. Lett. B* **629**, 20 (2005), arXiv:nucl-th/0411101.
- [5] F. Becattini, V. Chandra, L. Del Zanna, and E. Grossi, Relativistic distribution function for particles with spin at local thermodynamical equilibrium, *Annals Phys.* **338**, 32 (2013), arXiv:1303.3431 [nucl-th].
- [6] R.-h. Fang, L.-g. Pang, Q. Wang, and X.-n. Wang, Polarization of massive fermions in a vortical fluid, *Phys. Rev. C* **94**, 024904 (2016), arXiv:1604.04036 [nucl-th].
- [7] F. Becattini, L. Csernai, and D. J. Wang, Λ polarization in peripheral heavy ion collisions, *Phys. Rev. C* **88**, 034905 (2013), [Erratum: *Phys. Rev. C* 93,no.6,069901(2016)], arXiv:1304.4427 [nucl-th].
- [8] Y. Hidaka, S. Pu, and D.-L. Yang, Nonlinear Responses of Chiral Fluids from Kinetic Theory, *Phys. Rev. D* **97**, 016004 (2018), arXiv:1710.00278 [hep-th].
- [9] S. Y. F. Liu and Y. Yin, Spin Hall effect in heavy-ion collisions, *Phys. Rev. D* **104**, 054043 (2021), arXiv:2006.12421 [nucl-th].
- [10] S. Y. F. Liu and Y. Yin, Spin polarization induced by the hydrodynamic gradients, *JHEP* **07**, 188, arXiv:2103.09200 [hep-ph].
- [11] F. Becattini, M. Buzzegoli, and A. Palermo, Spin-thermal shear coupling in a relativistic fluid, *Phys. Lett. B* **820**, 136519 (2021), arXiv:2103.10917 [nucl-th].
- [12] B. Fu, S. Y. F. Liu, L. Pang, H. Song, and Y. Yin, Shear-Induced Spin Polarization in Heavy-Ion Collisions, *Phys. Rev. Lett.* **127**, 142301 (2021), arXiv:2103.10403 [hep-ph].
- [13] F. Becattini, M. Buzzegoli, G. Inghirami, I. Karpenko, and A. Palermo, Local Polarization and Isothermal Local Equilibrium in Relativistic Heavy Ion Collisions, *Phys. Rev. Lett.* **127**, 272302 (2021), arXiv:2103.14621 [nucl-th].
- [14] C. Yi, S. Pu, and D.-L. Yang, Reexamination of local spin polarization beyond global equilibrium in relativistic heavy ion collisions, *Phys. Rev. C* **104**, 064901 (2021), arXiv:2106.00238 [hep-ph].
- [15] S. Ryu, V. Jupic, and C. Shen, Probing early-time longitudinal dynamics with the Λ hyperon’s spin polarization in relativistic heavy-ion collisions, *Phys. Rev. C* **104**, 054908 (2021), arXiv:2106.08125 [nucl-th].
- [16] W. Florkowski, A. Kumar, A. Mazeliauskas, and R. Ryblewski, Effect of thermal shear on longitudinal spin polarization in a thermal model, *Phys. Rev. C* **105**, 064901 (2022), arXiv:2112.02799 [hep-ph].
- [17] B. Sahoo, C. R. Singh, and R. Sahoo, Estimating longitudinal polarization of Λ and $\bar{\Lambda}$ hyperons at relativistic energies using hydrodynamic and transport models, *Phys. Scripta* **100**, 065310 (2025), arXiv:2404.15138 [hep-ph].
- [18] J. Adam *et al.* (STAR), Polarization of Λ ($\bar{\Lambda}$) hyperons along the beam direction in Au+Au collisions at $\sqrt{s_{NN}} = 200$ GeV, *Phys. Rev. Lett.* **123**, 132301 (2019), arXiv:1905.11917 [nucl-ex].
- [19] S. Y. Liu, Y. Sun, and C. M. Ko, Spin Polarizations in a Covariant Angular-Momentum-Conserved Chiral Transport Model, *Phys. Rev. Lett.* **125**, 062301 (2020), arXiv:1910.06774 [nucl-th].
- [20] J.-A. Sun and L. Yan, Weak magnetic effect in quark-gluon plasma and local spin polarization*, *Chin. Phys. C* **49**, 071001 (2025), arXiv:2401.07458 [nucl-th].
- [21] C. Yi, X.-Y. Wu, J. Zhu, S. Pu, and G.-Y. Qin, Spin polarization of Λ hyperons along the beam direction in p+Pb collisions at $s_{NN}=8.16$ TeV using hydrodynamic approaches, *Phys. Rev. C* **111**, 044901 (2025), arXiv:2408.04296 [hep-ph].
- [22] A. Hayrapetyan *et al.* (CMS), Observation of Λ hyperon local polarization in pPb collisions at $\sqrt{s_{NN}} = 8.16$ TeV, *Phys. Rev. Lett.* **135**, 132301 (2025), arXiv:2502.07898 [nucl-ex].
- [23] S. Lin and Z. Wang, Shear induced polarization: collisional contributions, *JHEP* **12**, 030, arXiv:2206.12573 [hep-ph].
- [24] S. Fang, S. Pu, and D.-L. Yang, Quantum kinetic theory for dynamical spin polarization from QED-type interaction, *Phys. Rev. D* **106**, 016002 (2022), arXiv:2204.11519 [hep-ph].
- [25] S. Fang, S. Pu, and D.-L. Yang, Spin polarization and spin alignment from quantum kinetic theory with self-energy corrections, *Phys. Rev. D* **109**, 034034 (2024), arXiv:2311.15197 [hep-ph].
- [26] S. Lin and Z. Wang, Steady state, displacement current, and spin polarization for massless fermion in a shear flow, *Phys. Rev. D* **111**, 034032 (2025), arXiv:2406.10003 [hep-ph].
- [27] S. Fang and S. Pu, Collisional corrections to spin polarization from quantum kinetic theory using Chapman-Enskog expansion, *Phys. Rev. D* **111**, 034015 (2025), arXiv:2408.09877 [hep-ph].
- [28] S. Lin and J. Tian, Spin Polarized Quasi-particle in Off-equilibrium Medium (2024), arXiv:2410.22935 [hep-ph].

- [29] Z. Wang and S. Lin, Spin polarization for massive fermion in a shear flow: Complete results at $O(\partial)$, *Phys. Rev. D* **111**, 056023 (2025), [arXiv:2411.19550 \[hep-ph\]](#).
- [30] S. Fang, S. Pu, and D.-L. Yang, Radiative corrections on vortical spin polarization in hot QCD matter (2025), [arXiv:2503.13320 \[hep-ph\]](#).
- [31] N. Weickgenannt, D. Wagner, E. Speranza, and D. H. Rischke, Relativistic second-order dissipative spin hydrodynamics from the method of moments, *Phys. Rev. D* **106**, 096014 (2022), [arXiv:2203.04766 \[nucl-th\]](#).
- [32] N. Weickgenannt, D. Wagner, E. Speranza, and D. H. Rischke, Relativistic dissipative spin hydrodynamics from kinetic theory with a nonlocal collision term, *Phys. Rev. D* **106**, L091901 (2022), [arXiv:2208.01955 \[nucl-th\]](#).
- [33] N. Weickgenannt and J.-P. Blaizot, Spin kinetic theory with a nonlocal relaxation time approximation, *Phys. Rev. D* **111**, 056006 (2025), [arXiv:2409.11045 \[hep-ph\]](#).
- [34] D. Wagner, Resummed spin hydrodynamics from quantum kinetic theory, *Phys. Rev. D* **111**, 016008 (2025), [arXiv:2409.07143 \[nucl-th\]](#).
- [35] Sapna, S. K. Singh, and D. Wagner, Spin Polarization of Λ hyperons from Dissipative Spin Hydrodynamics (2025), [arXiv:2503.22552 \[hep-ph\]](#).
- [36] M. Stephanov and Y. Yin, Chiral Kinetic Theory, *Phys. Rev. Lett.* **109**, 162001 (2012), [arXiv:1207.0747 \[hep-th\]](#).
- [37] D. T. Son and N. Yamamoto, Berry Curvature, Triangle Anomalies, and the Chiral Magnetic Effect in Fermi Liquids, *Phys. Rev. Lett.* **109**, 181602 (2012), [arXiv:1203.2697 \[cond-mat.mes-hall\]](#).
- [38] J.-W. Chen, S. Pu, Q. Wang, and X.-N. Wang, Berry Curvature and Four-Dimensional Monopoles in the Relativistic Chiral Kinetic Equation, *Phys. Rev. Lett.* **110**, 262301 (2013), [arXiv:1210.8312 \[hep-th\]](#).
- [39] Y. Hidaka, S. Pu, and D.-L. Yang, Relativistic Chiral Kinetic Theory from Quantum Field Theories, *Phys. Rev. D* **95**, 091901 (2017), [arXiv:1612.04630 \[hep-th\]](#).
- [40] J.-H. Gao and Z.-T. Liang, Relativistic Quantum Kinetic Theory for Massive Fermions and Spin Effects, *Phys. Rev. D* **100**, 056021 (2019), [arXiv:1902.06510 \[hep-ph\]](#).
- [41] N. Weickgenannt, X.-L. Sheng, E. Speranza, Q. Wang, and D. H. Rischke, Kinetic theory for massive spin-1/2 particles from the Wigner-function formalism, *Phys. Rev. D* **100**, 056018 (2019), [arXiv:1902.06513 \[hep-ph\]](#).
- [42] K. Hattori, Y. Hidaka, and D.-L. Yang, Axial Kinetic Theory and Spin Transport for Fermions with Arbitrary Mass, *Phys. Rev. D* **100**, 096011 (2019), [arXiv:1903.01653 \[hep-ph\]](#).
- [43] Z. Wang, X. Guo, S. Shi, and P. Zhuang, Mass Correction to Chiral Kinetic Equations, *Phys. Rev. D* **100**, 014015 (2019), [arXiv:1903.03461 \[hep-ph\]](#).
- [44] S. Li and H.-U. Yee, Quantum Kinetic Theory of Spin Polarization of Massive Quarks in Perturbative QCD: Leading Log, *Phys. Rev. D* **100**, 056022 (2019), [arXiv:1905.10463 \[hep-ph\]](#).
- [45] D.-L. Yang, K. Hattori, and Y. Hidaka, Effective quantum kinetic theory for spin transport of fermions with collisional effects, *JHEP* **20**, 070, [arXiv:2002.02612 \[hep-ph\]](#).
- [46] N. Weickgenannt, E. Speranza, X.-L. Sheng, Q. Wang, and D. H. Rischke, Generating Spin Polarization from Vorticity through Nonlocal Collisions, *Phys. Rev. Lett.* **127**, 052301 (2021), [arXiv:2005.01506 \[hep-ph\]](#).
- [47] Z. Wang, X. Guo, and P. Zhuang, Equilibrium Spin Distribution From Detailed Balance, *Eur. Phys. J. C* **81**, 799 (2021), [arXiv:2009.10930 \[hep-th\]](#).
- [48] K. Hattori, Y. Hidaka, N. Yamamoto, and D.-L. Yang, Wigner functions and quantum kinetic theory of polarized photons, *JHEP* **02**, 001, [arXiv:2010.13368 \[hep-ph\]](#).
- [49] Y. Hidaka, S. Pu, Q. Wang, and D.-L. Yang, Foundations and applications of quantum kinetic theory, *Prog. Part. Nucl. Phys.* **127**, 103989 (2022), [arXiv:2201.07644 \[hep-ph\]](#).
- [50] D. Montenegro, L. Tinti, and G. Torrieri, Ideal relativistic fluid limit for a medium with polarization, *Phys. Rev. D* **96**, 056012 (2017), [Addendum: *Phys. Rev. D* **96**, no.7, 079901 (2017)], [arXiv:1701.08263 \[hep-th\]](#).
- [51] W. Florkowski, B. Friman, A. Jaiswal, and E. Speranza, Relativistic fluid dynamics with spin, *Phys. Rev. C* **97**, 041901 (2018), [arXiv:1705.00587 \[nucl-th\]](#).
- [52] W. Florkowski, R. Ryblewski, and A. Kumar, Relativistic hydrodynamics for spin-polarized fluids, *Prog. Part. Nucl. Phys.* **108**, 103709 (2019), [arXiv:1811.04409 \[nucl-th\]](#).
- [53] D.-L. Yang, Side-Jump Induced Spin-Orbit Interaction of Chiral Fluids from Kinetic Theory, *Phys. Rev. D* **98**, 076019 (2018), [arXiv:1807.02395 \[nucl-th\]](#).
- [54] K. Hattori, M. Hongo, X.-G. Huang, M. Matsuo, and H. Taya, Fate of spin polarization in a relativistic fluid: An entropy-current analysis, *Phys. Lett. B* **795**, 100 (2019), [arXiv:1901.06615 \[hep-th\]](#).
- [55] K. Fukushima and S. Pu, Spin hydrodynamics and symmetric energy-momentum tensors – A current induced by the spin vorticity –, *Phys. Lett. B* **817**, 136346 (2021), [arXiv:2010.01608 \[hep-th\]](#).
- [56] S. Shi, C. Gale, and S. Jeon, From chiral kinetic theory to relativistic viscous spin hydrodynamics, *Phys. Rev. C* **103**, 044906 (2021), [arXiv:2008.08618 \[nucl-th\]](#).
- [57] S. Li, M. A. Stephanov, and H.-U. Yee, Nondissipative Second-Order Transport, Spin, and Pseudogauge Transformations in Hydrodynamics, *Phys. Rev. Lett.* **127**, 082302 (2021), [arXiv:2011.12318 \[hep-th\]](#).
- [58] M. Hongo, X.-G. Huang, M. Kaminski, M. Stephanov, and H.-U. Yee, Relativistic spin hydrodynamics with torsion and linear response theory for spin relaxation, *JHEP* **11**, 150, [arXiv:2107.14231 \[hep-th\]](#).
- [59] S. Bhadury, W. Florkowski, A. Jaiswal, A. Kumar, and R. Ryblewski, Relativistic Spin Magnetohydrodynamics, *Phys. Rev. Lett.* **129**, 192301 (2022), [arXiv:2204.01357 \[nucl-th\]](#).
- [60] S. Acharya *et al.* (ALICE), Evidence of Spin-Orbital Angular Momentum Interactions in Relativistic Heavy-Ion Collisions, *Phys. Rev. Lett.* **125**, 012301 (2020), [arXiv:1910.14408 \[nucl-ex\]](#).
- [61] M. S. Abdallah *et al.* (STAR), Pattern of global spin alignment of ϕ and K^{*0} mesons in heavy-ion collisions, *Nature* **614**, 244 (2023), [arXiv:2204.02302 \[hep-ph\]](#).
- [62] X.-L. Sheng, L. Oliva, Z.-T. Liang, Q. Wang, and X.-N. Wang, Spin Alignment of Vector Mesons in Heavy-Ion Collisions, *Phys. Rev. Lett.* **131**, 042304 (2023), [arXiv:2205.15689 \[nucl-th\]](#).
- [63] X.-L. Sheng, L. Oliva, Z.-T. Liang, Q. Wang, and X.-N. Wang, Relativistic spin dynamics for vector mesons, *Phys. Rev. D* **109**, 036004 (2024), [arXiv:2206.05868 \[hep-ph\]](#).
- [64] X.-L. Sheng, S. Pu, and Q. Wang, Momentum dependence of the spin alignment of the ϕ meson, *Phys. Rev. C* **108**, 054902 (2023), [arXiv:2308.14038 \[nucl-th\]](#).
- [65] A. Kumar, B. Müller, and D.-L. Yang, Spin polarization

- and correlation of quarks from the glasma, *Phys. Rev. D* **107**, 076025 (2023), [arXiv:2212.13354 \[nucl-th\]](#).
- [66] A. Kumar, B. Müller, and D.-L. Yang, Spin alignment of vector mesons by glasma fields, *Phys. Rev. D* **108**, 016020 (2023), [arXiv:2304.04181 \[nucl-th\]](#).
- [67] D.-L. Yang, Transverse and longitudinal spin alignment from color fields in heavy ion collisions, *Phys. Rev. D* **111**, 056005 (2025), [arXiv:2411.14822 \[nucl-th\]](#).
- [68] B. Müller and D.-L. Yang, Anomalous spin polarization from turbulent color fields, *Phys. Rev. D* **105**, L011901 (2022), [arXiv:2110.15630 \[nucl-th\]](#).
- [69] D.-L. Yang, Quantum kinetic theory for spin transport of quarks with background chromo-electromagnetic fields, *JHEP* **06**, 140, [arXiv:2112.14392 \[hep-ph\]](#).
- [70] M. E. Carrington, S. Mrowczynski, and J.-Y. Ollitrault, Hydrodynamic-like behavior of glasma, *Phys. Rev. C* **110**, 054903 (2024), [arXiv:2406.14463 \[nucl-th\]](#).
- [71] L. D. McLerran and R. Venugopalan, Computing quark and gluon distribution functions for very large nuclei, *Phys. Rev. D* **49**, 2233 (1994), [arXiv:hep-ph/9309289](#).
- [72] L. D. McLerran and R. Venugopalan, Gluon distribution functions for very large nuclei at small transverse momentum, *Phys. Rev. D* **49**, 3352 (1994), [arXiv:hep-ph/9311205](#).
- [73] L. D. McLerran and R. Venugopalan, Green's functions in the color field of a large nucleus, *Phys. Rev. D* **50**, 2225 (1994), [arXiv:hep-ph/9402335](#).
- [74] F. Gelis, E. Iancu, J. Jalilian-Marian, and R. Venugopalan, The Color Glass Condensate, *Ann. Rev. Nucl. Part. Sci.* **60**, 463 (2010), [arXiv:1002.0333 \[hep-ph\]](#).
- [75] J. L. Albacete and C. Marquet, Gluon saturation and initial conditions for relativistic heavy ion collisions, *Prog. Part. Nucl. Phys.* **76**, 1 (2014), [arXiv:1401.4866 \[hep-ph\]](#).
- [76] T. Lappi and L. McLerran, Some features of the glasma, *Nucl. Phys. A* **772**, 200 (2006), [arXiv:hep-ph/0602189](#).
- [77] T. Lappi, Energy density of the glasma, *Phys. Lett. B* **643**, 11 (2006), [arXiv:hep-ph/0606207](#).
- [78] B. Schenke, S. Jeon, and C. Gale, (3+1)D hydrodynamic simulation of relativistic heavy-ion collisions, *Phys. Rev. C* **82**, 014903 (2010), [arXiv:1004.1408 \[hep-ph\]](#).
- [79] A. Kumar, D.-L. Yang, and P. Gubler, Spin alignment of vector mesons by second-order hydrodynamic gradients, *Phys. Rev. D* **109**, 054038 (2024), [arXiv:2312.16900 \[nucl-th\]](#).
- [80] G. Chen and R. J. Fries, Global Flow of Glasma in High Energy Nuclear Collisions, *Phys. Lett. B* **723**, 417 (2013), [arXiv:1303.2360 \[nucl-th\]](#).
- [81] G. Chen, R. J. Fries, J. I. Kapusta, and Y. Li, Early Time Dynamics of Gluon Fields in High Energy Nuclear Collisions, *Phys. Rev. C* **92**, 064912 (2015), [arXiv:1507.03524 \[nucl-th\]](#).
- [82] K. J. Golec-Biernat and M. Wusthoff, Saturation effects in deep inelastic scattering at low Q^2 and its implications on diffraction, *Phys. Rev. D* **59**, 014017 (1998), [arXiv:hep-ph/9807513](#).
- [83] P. Guerrero-Rodríguez and T. Lappi, Evolution of initial stage fluctuations in the glasma, *Phys. Rev. D* **104**, 014011 (2021), [arXiv:2102.09993 \[hep-ph\]](#).
- [84] J. S. Schwinger, On gauge invariance and vacuum polarization, *Phys. Rev.* **82**, 664 (1951).
- [85] N. K. Glendenning and T. Matsui, CREATION OF ANTI-Q Q PAIR IN A CHROMOELECTRIC FLUX TUBE, *Phys. Rev. D* **28**, 2890 (1983).
- [86] A. K. Kerman, T. Matsui, and B. Svetitsky, Particle Production in the Central Rapidity Region of Ultrarelativistic Nuclear Collisions, *Phys. Rev. Lett.* **56**, 219 (1986).
- [87] G. Gatoff, A. K. Kerman, and T. Matsui, The Flux Tube Model for Ultrarelativistic Heavy Ion Collisions: Electrohydrodynamics of a Quark Gluon Plasma, *Phys. Rev. D* **36**, 114 (1987).
- [88] N. Tanji, Quark pair creation in color electric fields and effects of magnetic fields, *Annals Phys.* **325**, 2018 (2010), [arXiv:1002.3143 \[hep-ph\]](#).
- [89] H. Taya, Quark and Gluon Production from a Boost-invariantly Expanding Color Electric Field, *Phys. Rev. D* **96**, 014033 (2017), [arXiv:1609.06189 \[nucl-th\]](#).
- [90] W. Florkowski, A. Kumar, R. Ryblewski, and A. Mazeliauskas, Longitudinal spin polarization in a thermal model, *Phys. Rev. C* **100**, 054907 (2019), [arXiv:1904.00002 \[nucl-th\]](#).
- [91] W. Broniowski and W. Florkowski, Explanation of the RHIC p(T) spectra in a thermal model with expansion, *Phys. Rev. Lett.* **87**, 272302 (2001), [arXiv:nucl-th/0106050](#).
- [92] Y. Kanakubo, Y. Tachibana, and T. Hirano, Interplay between core and corona components in high-energy nuclear collisions, *Phys. Rev. C* **105**, 024905 (2022), [arXiv:2108.07943 \[nucl-th\]](#).
- [93] P. B. Arnold, G. D. Moore, and L. G. Yaffe, Effective kinetic theory for high temperature gauge theories, *JHEP* **01**, 030, [arXiv:hep-ph/0209353](#).
- [94] A. Kurkela and Y. Zhu, Isotropization and hydrodynamization in weakly coupled heavy-ion collisions, *Phys. Rev. Lett.* **115**, 182301 (2015), [arXiv:1506.06647 \[hep-ph\]](#).
- [95] A. Kurkela, A. Mazeliauskas, J.-F. Paquet, S. Schlichting, and D. Teaney, Matching the Nonequilibrium Initial Stage of Heavy Ion Collisions to Hydrodynamics with QCD Kinetic Theory, *Phys. Rev. Lett.* **122**, 122302 (2019), [arXiv:1805.01604 \[hep-ph\]](#).
- [96] X.-G. Huang, An introduction to relativistic spin hydrodynamics, *Nucl. Sci. Tech.* **36**, 208 (2025), [arXiv:2411.11753 \[nucl-th\]](#).